

Supporting Online Material

Subjects: The animals in this study were *Bmal1*^{-/-} mice, originally generated in the C. Bradfield laboratory (5) and obtained from C. Weitz. They were housed in the Harvard Animal Research Facility and the care of animals used in this study met National Institutes of Health standards, as set forth in the *Guide for the Care and Use of Laboratory Animals* and was approved by the Beth Israel Deaconess Medical Center and Harvard Medical School Institutional Animal Care and Use Committees.

Biotelemetry Surgery, Brain Injections and Recordings: All mice were implanted i.p. with biotelemetry transmitters (TA10TA-F20; Data Sciences International) to record body temperature (T_b) and locomotor activity (LMA). All animals were anesthetized (3% isofluorane in pure medical-grade oxygen), a midline celiotomy was performed, and a sterilized transmitter was inserted into the peritoneal cavity with aseptic technique. Immediately following the implant procedure, all mice received bilateral stereotaxic injections of recombinant AAV-BMAL1, AAV-GFP or saline into the SCN or DMH with a glass micropipette and air pressure injection system. All incisions were sutured and treated with a topical antibiotic, and all animals received flunixin as an analgesic for 48 hrs during recovery.

The mice recovered from surgery for 14 days before recording of T_b and LMA began. The animals were individually housed in standard plastic mouse cages with ad libitum food (Lab Diet) and water. Each cage was placed on top of a telemetry receiver interfaced

to a microcomputer data acquisition system (Data Sciences). T_b values were recorded at 5-min intervals, and activity data were collected in 5-min bins. The cages were housed inside isolation chambers, which provided ventilation, a computer-controlled lighting regimen, an ambient temperature of $22 \pm 1^\circ\text{C}$, and visual isolation. Cages were changed every other week and health checks were performed daily by real-time analysis of the telemetry data; thus, the mice were not disturbed during the daily health checks. A white-light LED matrix provided ambient environmental lighting. The white light was produced by an array of 18 single LEDs (light peak 490/540nm) using a phosphor layer (Yttrium Aluminum Garnet) on the surface of a blue (Gallium Nitride) chip (The LED Light, Inc.).

Restricted Feeding: In the first experiment, we examined food entrainment in a 12:12 light-dark cycle (LD). Following surgical recovery, mice were provided food ad libitum in LD (lights on = ZT0) for 2-3 weeks. The mice were then challenged with restricted feeding for 2 weeks with a daily 4-h meal presented ZT4. The restricted feeding period was followed by a 1-d food deprivation period to assess the T_b and LMA rhythms in the absence of the daily feeding stimulus. Mice were killed at the end of the food deprivation period.

In the second experiment, we examined food entrainment in constant darkness (DD). Following surgical recovery, mice were provided food ad libitum in DD for 2-3 weeks. The mice were then challenged with restricted feeding for 2 weeks in DD with a daily 4-h meal presented CT4. Behavioral observation and health checks were performed using

night-vision goggles. The restricted feeding period was followed by a 1-d food deprivation period to assess the activity and body temperature rhythms in the absence of the daily feeding stimulus. Mice were killed at the end of the food deprivation period.

Mice faced with restricted food access may use the strategy of torpor, in which they fall into a hibernation-like state for part of the day when no food is expected (1). These periods of hypothermia ($<31^{\circ}\text{C}$ T_b) and behavioral inactivity alternate with periods of wakefulness and foraging behavior (locomotion). When mice are tested for food entrainment under LD conditions, they may go into torpor during the night (when they would otherwise be awake) and forage more consistently during the day. However, this appearance of “food entrainment” may be a response to the light cue (i.e., the animals learn that food is available when the light is on, and sleep more when the light is off) rather than a circadian rhythm. Moreover, and somewhat paradoxically, rodents demonstrate increased spontaneous wheel running activity (during the light phase) under reduced caloric conditions (2), presumably representing foraging behavior. We therefore tested *Bmal1*^{-/-} mice for food entrainment under DD conditions, so that bouts of torpor, when they occurred, were not cued by the light-dark cycle.

AAV-BMAL1 cassette: PCR was used to amplify and then clone a 1kb *Bmal1*-promoter fragment from genomic DNA (3), FLAG/HA double tag from pOZ-N (3), mouse *Bmal1* cDNA, and *Bmal1* 3' UTR/flanking sequence from mouse genomic DNA. All fragments were verified by sequencing and then cloned in subsequent steps to yield the plasmid pBS-endo-FH/Bmal1. The final composed expression cassette was essentially as

described by Nagoshi et al (4), except that it drives FLAG/HA-BMAL1 expression. The cassette was excised from pBS-endo-FH/Bmal1 via NotI digestion and subcloned into AAV viral DNA (serotype 8) to generate AAV expressing FLAG/HA-BMAL1. The virus was generated by tripartite transfection (AAV-rec/cap expression plasmid, adenovirus miniplasmid and AAV vector plasmid) into 293A cells and purified by iodixanol gradient. The eluted virus was dialyzed against PBS and titered by dot blot hybridization (3.1×10^{13} /ml).

In situ hybridization: *Bmal1*, *Per1* and *Per2* expression were monitored by using ^{35}S -labeled riboprobes. Plasmids were linearized and transcribed with T3 polymerases to produce antisense RNA probes that were ^{35}S -radiolabeled. Sections were mounted and hybridization was performed as described (5). Probes were visualized by dipping the slides in photographic emulsion, allowing 2-4 weeks for exposure, and then developing in Kodak D-19, fixing, drying, and coverslipping the slides. Clock gene expression was quantified at a magnification of x20 under darkfield illumination from the emulsion-coated sections of the SCN and DMH. Briefly, digital photomicrographs were acquired with Zeiss Axiovision 4.5 software. The images of the SCN and DMH were adjusted for optimal display of the minimum and maximum contained grey values and then imported into ImageJ 1.37 to calculate the mean optical density of *Bmal1*-, *Per1*- and *Per2*-positive neurons.

Circadian Analysis: Period analysis was performed using a Linear/Non-Linear Least-Squares Cosine Fit Spectral Analysis (L/NL SA), which was originally described by Rummel and coworkers (6). This spectral analysis routine combines linear and non-linear cosine fits to a data set along with iterative optimization of significant periods. The results of the L/NL SA were then compared with the results of a periodogram analysis. The periodogram analysis, originally described by Enright (7), provided a period estimate by dividing the data set into windows of differing lengths and then calculated the average variance for each window length (i.e., period). The period or window with the greatest average variance is taken to best approximate the natural period of the data set. Results of the period analysis were consistent within an animal between the L/NL SA and periodogram techniques.

Statistical Analysis: A two factor repeated measures ANOVA was used to compare rhythm period, mean and amplitude between lighting and genotype conditions. Specific mean comparisons were made using Tukey's HSD post hoc test (SPSS). An $\alpha < 0.01$ was used for all tests. All data are reported as mean \pm standard deviation.

Supplementary References

1. G.P. Webb, S.A. Jagot, M.E. Jakobson, *Comp. Biochem. Physiol.* 72 (1982).
2. Hebebrand, C. et al., *Physiol. Behav.* 79 (2003).
3. Nakatani Y and Ogryzko V, *Methods Enzymology* (2003).
4. Nagoshi et al., *Cell* 5, 119 (2004).

5. Gooley et al., Nat. Neurosci. 4, 1165 (2001).
6. Rummel JA. Biorhythms and Human Reproduction (1974).
7. Enright J T J. Theor. Biol. 8:426-468 (1965).

SUPPLEMENTARY FIGURES

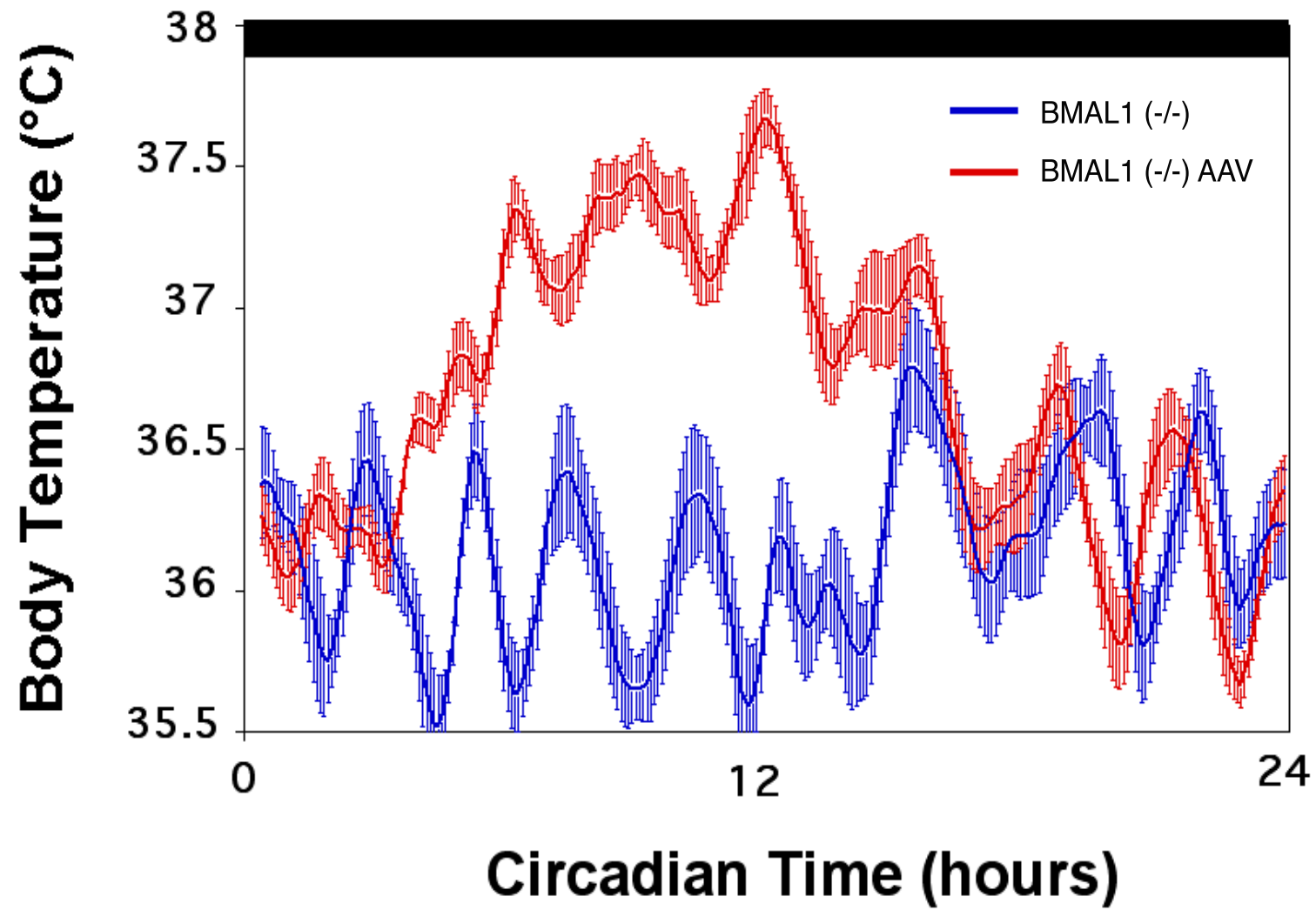
Supplementary Figure 1. AAV-BMAL1 injection into the SCN rescues the light-entrainable circadian rhythm in body temperature (T_b). T_b waveform (mean \pm SEM T_b from days 21-27 of DD) of the circadian T_b rhythm during ad lib feeding for an individual *Bmal1*^{-/-} mouse (blue trace) and an individual *Bmal1*^{-/-} mouse (red trace) following bilateral AAV-BMAL1 injections into the SCN. Whereas *Bmal1*^{-/-} mice demonstrated only a persisting ultradian pattern of T_b , *Bmal1*^{-/-} mice with bilateral SCN injections of AAV-BMAL1 exhibited a high amplitude, free-running T_b rhythm with substantial damping of the ultradian components.

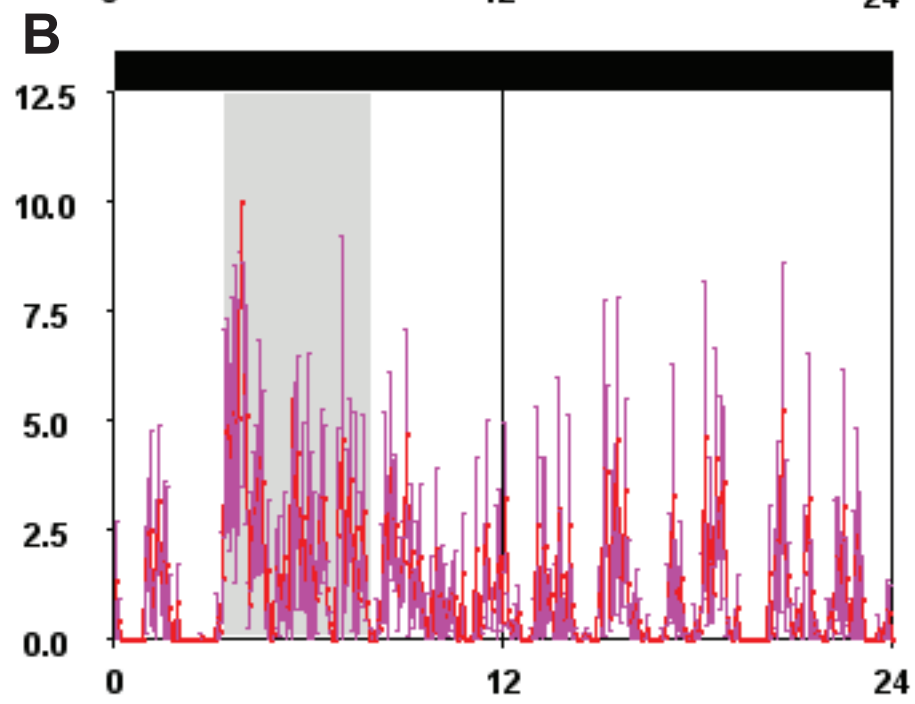
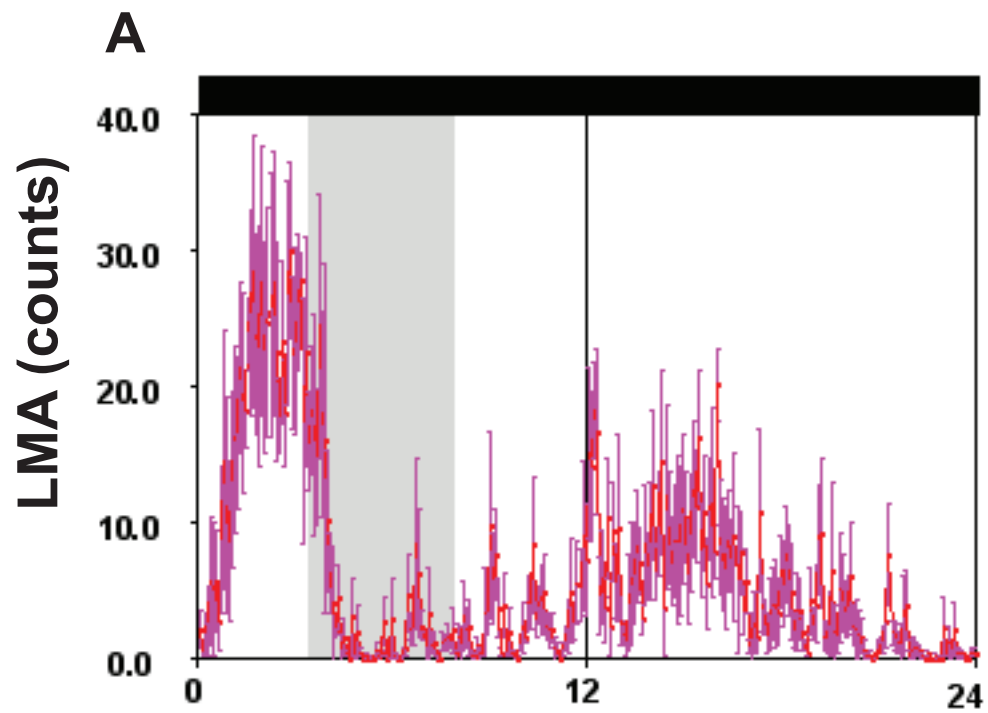
Supplementary Figure 2. Food entrainment of the locomotor activity (LMA) rhythm is rescued by AAV-BMAL1 injection into the DMH. Under DD conditions, *Bmal1*^{+/-} and *Bmal1*^{-/-} mice were placed under restricted feeding (RF) for 2 weeks (food available from CT4-8, gray vertical bar in A-C). Shown in supplementary Figure 2A-C are the waveforms (mean \pm SEM) for LMA on days 10-14 of RF for an individual mouse. (A) *Bmal1*^{+/-} but not (B) *Bmal1*^{-/-} mice demonstrated a clear rise in LMA ~2-3 hours preceding food availability under RF. It can further be seen in (B) that the *Bmal1*^{-/-} mice often demonstrated zero LMA in the 1-2 hours preceding food availability, requiring rousing by the investigator to avoid starvation. (C) Following bilateral injection of AAV-BMAL1 into the DMH of *Bmal1*^{-/-} mice, food entrainment was rescued as indicated by the preprandial elevation in LMA. Note the ordinate scale for (B and C) is

expanded with respect to (A) because of the significantly lower ($p < 0.001$) LMA levels of the *Bmal1*^{-/-} mice and AAV-*Bmal1*^{-/-} mice.

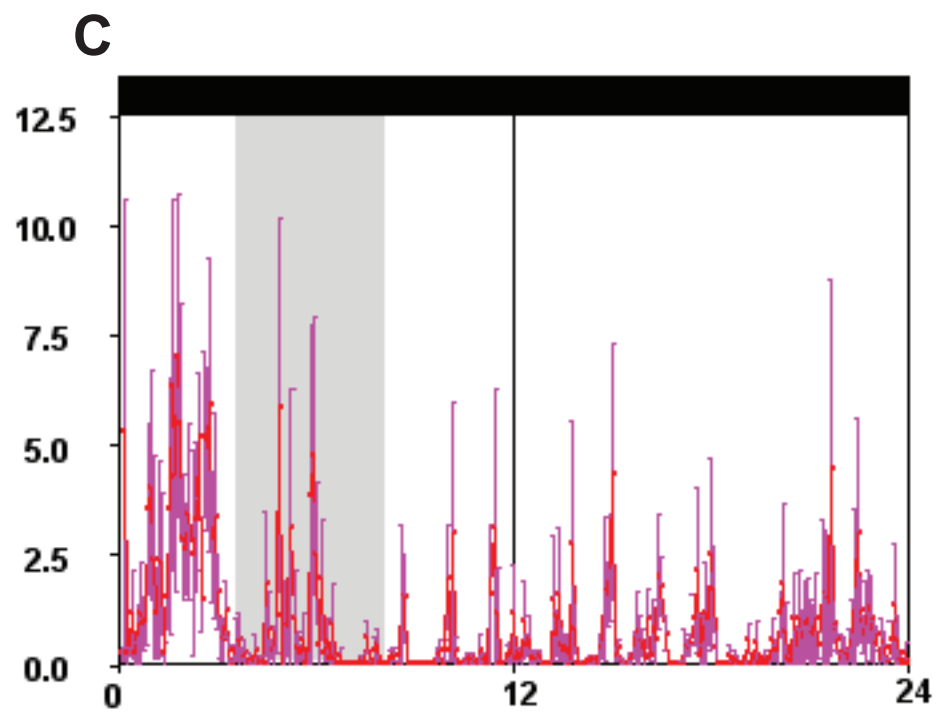
Supplementary Figure 3. Food entrainment of the body temperature (T_b) rhythm is not rescued by AAV-BMAL1 injections into the SCN. Under DD conditions, *Bmal1*^{+/-} and *Bmal1*^{-/-} mice (with AAV-BMAL1 injections into the SCN) were placed under restricted feeding (RF) for 2 weeks. (A) *Bmal1*^{+/-} mice demonstrated a clear rise in T_b ~2-3 hours preceding food availability under RF (red line in A and B = onset of food availability). (B) Bilateral injection of AAV-BMAL1 into the SCN of *Bmal1*^{-/-} mice did not rescue food entrainment as indicated by the lack of a preprandial elevation in T_b . (C-D) are the waveforms (mean \pm SEM) for T_b on days 10-14 of RF for the individual mice shown in (A) and (B), respectively (food available from CT4-8, gray vertical bar in C-D).

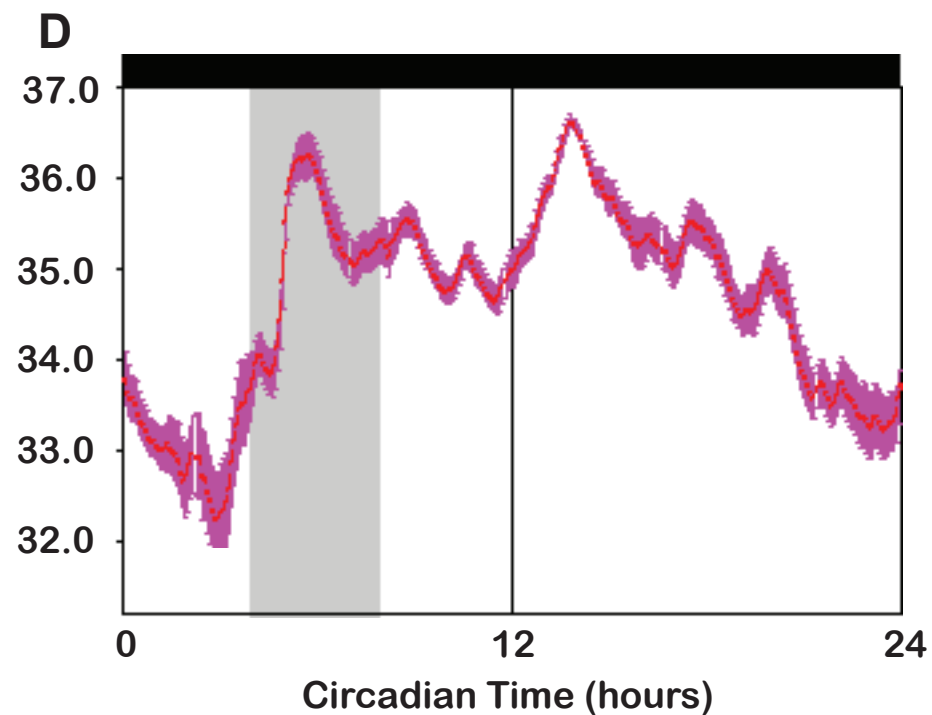
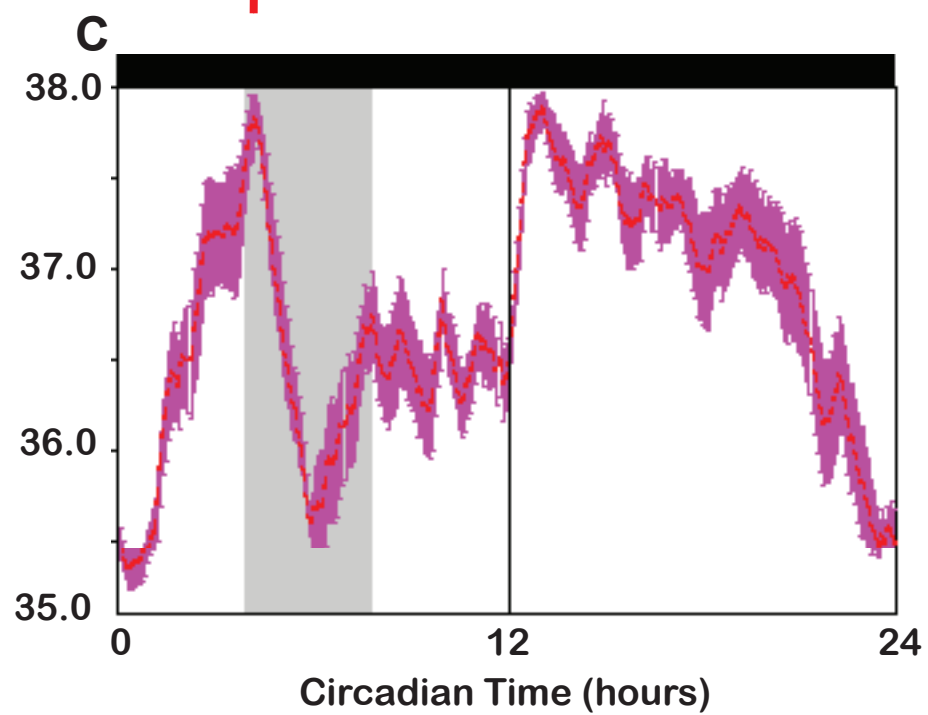
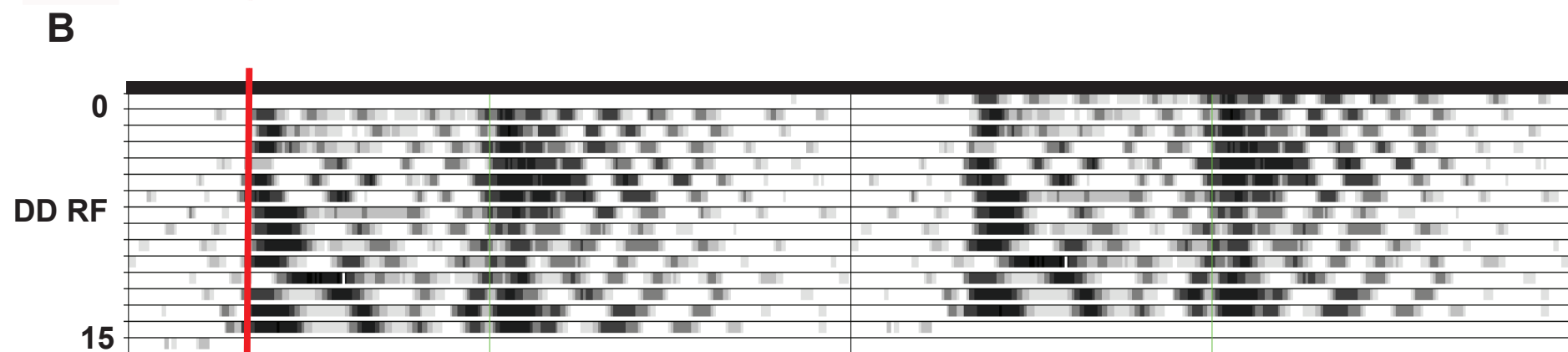
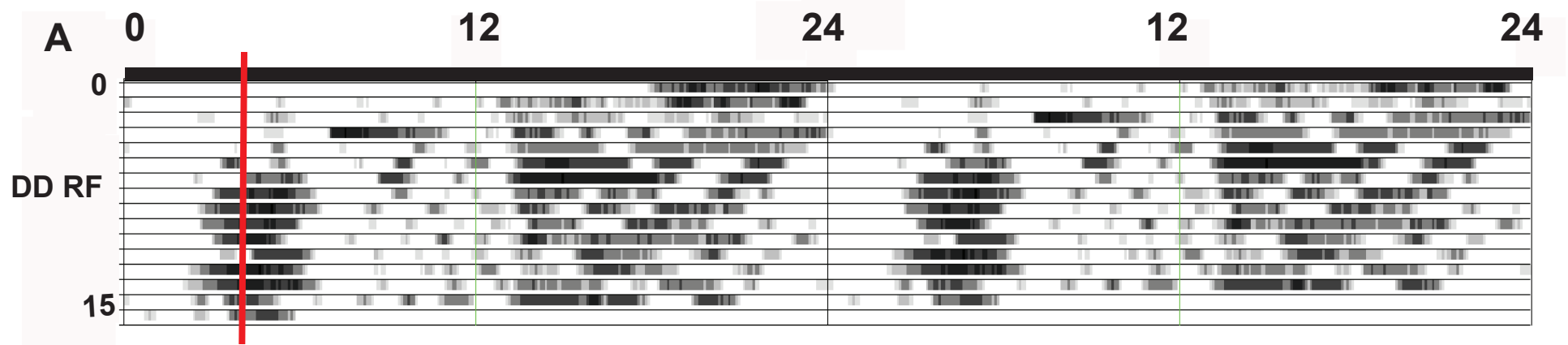
Supplementary Figure 4. *Per1* expression in the SCN of (A) *Bmal1*^{+/-} mice, (B) *Bmal1*^{-/-} mice and (C) *Bmal1*^{-/-} mice with AAV-BMAL1 injections into the SCN (all at ZT6 and under ad lib feeding conditions). (D) *Bmal1* expression in the SCN of *Bmal1*^{-/-} mice with AAV-BMAL1 injections (ZT18, under ad lib feeding conditions). *Per1* expression in the DMH of (E) *Bmal1*^{+/-} mice, (F) *Bmal1*^{-/-} mice and (G) *Bmal1*^{-/-} mice with AAV-BMAL1 injections into the DMH (all at ZT6; E is ad lib feeding and F, G under restricted feeding conditions). (H) *Bmal1* expression in the DMH of *Bmal1*^{-/-} mice with AAV-BMAL1 injections (ZT18, under restricted feeding conditions).





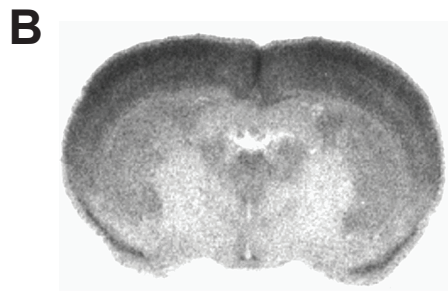
Circadian Time (hours)



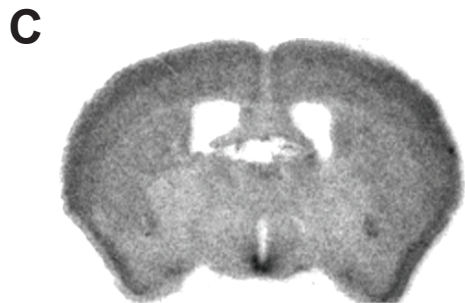




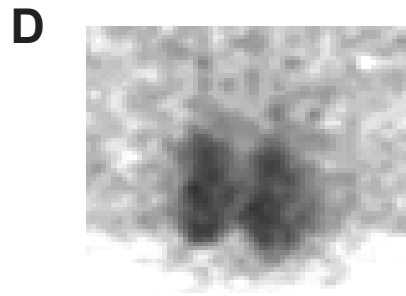
ZT 6 *Bmal* +/−



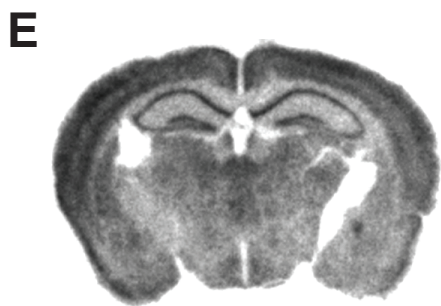
ZT 6 *Bmal* −/−



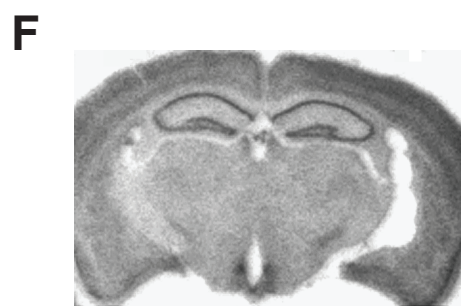
ZT 6 AAV *Bmal* −/−



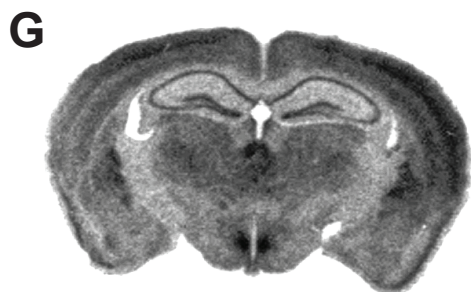
ZT 18 AAV *Bmal* −/−



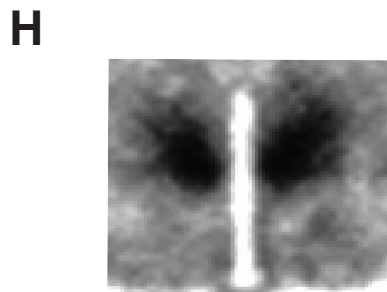
ZT 6 *Bmal* +/−



ZT 6 *Bmal* −/−



ZT 6 AAV *Bmal* −/−



ZT 18 AAV *Bmal* −/−